# Assessment of Forest Transitions
## and Regions of Conservation
## Importance in Udupi district, Karnataka

*The current study prioritizes regions of conservation importance at the disaggregated level in the Udupi district, Central Western Ghats, based on ecological, geo-climatic, land, and social aspects. Conservation importance regions (CIR) or Ecological Sensitive Regions (ESR) are the distinct ecological units with exceptional biotic and abiotic elements which need at most care and sustainable development. CIR prioritization at grid levels (5'x5' grids or 9x9 km) acts as a spatial decision support system to better understand the forest landscape dynamics and planning. The analyses of forest landscape dynamics using the temporal remote sensing data in reveal an increase in built-up areas by 8.8% with a decline in forest cover, resulting in the rise in maximum temperature by $4^0C$ in Udupi district during 1990-2018. Multivariate statistical analysis is done to understand the role of landscape dynamics on the land surface temperature (LST). The correlation analysis shows an increasing trend of LST across the CIR region with r= 0.8 where CIR 1 indicates the lowest temperature and CIR 4 has the maximum temperature.*

**Introduction**

Forests constitute vital ecosystems covering about 30% of the Earth's surface. Forest cover changes, especially due to unplanned anthropogenic activities (Huang *et al.*, 2008), have widespread effects on the provision of ecosystem services towards human welfare (Lawrence and Vandecar, 2015; Ramachandra *et al.*, 2020). As pressure on forest cover increases due to human interventions, there has been a growing concern to mitigate deforestation through monitoring at global and regional scales (Aronson and Alexander, 2013; Kuemmerle *et al.*, 2009). Vegetation in the forest ecosystem plays a significant role in mitigating carbon in the atmosphere through sequestration during photosynthesis (Hansen *et al.*, 2010; Ramachandra and Bharath, 2019a). Forests provide ecological, economic, and social services to human society, including the provision of food, refuges for biodiversity, regulation of the hydrologic cycle, medicinal and forest products, recreational uses, protection of soil resources, and spiritual needs. Forests play a decisive role in the hydrologic cycle through evapotranspiration which moderates climate through feedbacks from clouds and precipitation. The ratio of evapotranspiration to available energy is relatively lower in regions with native forests compared to croplands or monoculture plantations (Bonan, 2008). Vegetation cover in forests is due to the long-term interaction of geomorphological features, hydrological conditions, soil type, climate

*Conservation importance regions in Udupi district, central Western Ghats*

***T.V. RAMACHANDRA***[1,2,3,]
***BHARATH SETTURU***[1] ***AND S. VINAY***[1]
*E-mail: tvr@iisc.ac.in*

[1]Energy and Wetlands Research Group, Center for Ecological Sciences [CES], Indian Institute of Science
[2]Centre for Sustainable Technologies (astra)
[3]Centre for infrastructure, Sustainable Transportation and Urban Planning [CiSTUP], Indian Institute of Science, Bangalore, Karnataka, 560 012, India

change, and anthropogenic activities (Zhu *et al*., 2012). It helps in modulating the ecosystem through water retention, atmospheric circulation, and terrestrial soil stability and maintains the balance of an ecosystem (Liu *et al*., 2009; Leilei *et al*., 2014). Therefore, quantification of spatial extent and conditions of a forest ecosystem provides insights into changes that will aid natural resources management (Hansen *et al*., 2000).

Forest landscape transitions involving the degradation of forests have increased land surface temperature (LST), which is the radiative skin temperature of the earth's surface. It is one of the key elements representing the integrated features of land-atmosphere physical and dynamic processes (Shwetha and Kumar, 2016). LST and emissivity aid in understanding energy budget estimation '(Chakraborty *et al*., 2015; Mohamed *et al*., 2017; Liang *et al*., 2019). Emissivity is the ratio of energy radiated from a material's surface to that radiated from a blackbody (a perfect emitter) at the same temperature and wavelength at the same viewing conditions. The emissivity of a surface depends not only on the material but also on the nature of the surface. Estimating LST using emissivity as a parameter provides accurate information with appropriate calibration of LULC changes (Bharath *et al*., 2013). Conventionally, LST is measured from the direct ground measurement. LST is estimated using the data of thermal infrared bands with the advancement in satellite remote sensing, by either split-window algorithms or mono window algorithms or radiative transfer equation (Le-Xiang *et al*., 2006; Jackson and Baker, 2010; Asgarian *et al*., 2015; Kayet *et al*., 2016; Estoque *et al*., 2017; Kumari *et al*., 2018; Mujabar and Rao, 2018; Ramachandra *et al*., 2018b; Danodia *et al*., 2019). Urbanization is a dominant demographic trend, marked by the process of change in land use, causing the transition from a rural to a more urban society. As an increment in urban landuse, it reflects the loss of vegetation, agricultural land, open space, etc. This has prompted investigation of the causes and consequences of LULC by mapping and modeling landscape patterns and dynamics - (Ramachandra and Kumar, 2010; Ramachandra and Bharath, 2019c). Hence, forest transition analysis has become a prerequisite for managing and monitoring ecosystem and environmental changes.

Humans depend either directly or indirectly on forests to the extent of 80% in the developing world. Altering the ecological integrity would impact the ecological goods and services, affecting the livelihood of the dependent population (Ramachandra *et al*., 2017). The conservation and sustainable management of ecosystems are vital components in pursuing ecologically sound, economically viable, and socially acceptable development goals (Xianhong, 2015;

Ramachandra *et al*., 2018, 2021). This entails identifying regions of conservation importance. Regions of conservation importance refer to ecologically sensitive regions (ESR) or ecologically fragile areas for their ecological, biological, cultural, economic and historical values and are conserved by government regulations (Gadgil *et al*., 2011). Conservation importance regions (CIR) or ESR refers to the zones of permanent and irreparable loss of extant life forms or significant damage to the natural processes of evolution and speciation with the alterations in the ecological integrity of a region. CIR demarcation reflects the scope for different environmental regulations, management issues, and social realities. It acts as a decision-making framework to understand the region's biodiversity, stakeholders and strategies necessitate for protection, which aids in solving livelihood issues (Ramachandra *et al*., 2017). The increased exploitation of natural resources and large-scale landscape transformations have led to the degradation of the ecosystem. The decision-making process should mandatorily include the conservation of intact ecosystems to ensure the sustenance of natural resources to meet the present and future needs (Ramachandra *et al*., 2016). The main objective of the current study is to prioritize CIRs in Udupi district (central Western Ghats), Karnataka State, India, and understand the linkages of LST with LU and CIR.

**Material and Methods**

*Study area*

Udupi district (13°04' and 13°59' N latitude and 74°35' and 75°12' E longitude) was formed in the year 1997 with three taluks *i.e*., Udupi, Kundapur, and Karkala from the undivided parent district of Dakshina Kannada. The district is bounded by Uttara Kannada district in north and Dakshina Kannada district in southern direction with 3582 km$^2$ geographical area (Fig. 1). The district is blessed with abundant rainfall, fertile soil, and lush vegetation. The slopes of the Western Ghats are endowed with dense forests containing valuable species, including timber and fuelwood. The soils of the district are drained by perennial rivers such as Varahi, Gangolli, Sitandi, and Swarna, which join the Arabian Sea, known for its estuarine diversity. Udupi district gets an annual rainfall of 4000 mm. The climate is marked by heavy rainfall, high humidity, and sticky weather in the hot seasons. Pristine beaches, picturesque mountain ranges, temple towns, and rich culture make it a famous tourist destination. It is well known for Yakshagana- a fabulous costumed dance-drama form, Kambala- the buffalo racing sport by farmers, Kori-Katta (Cock Fight), and Bootha Kola. The district has witnessed large scale developmental activities post-2000 (Ramachandra and Aithal, 2012).
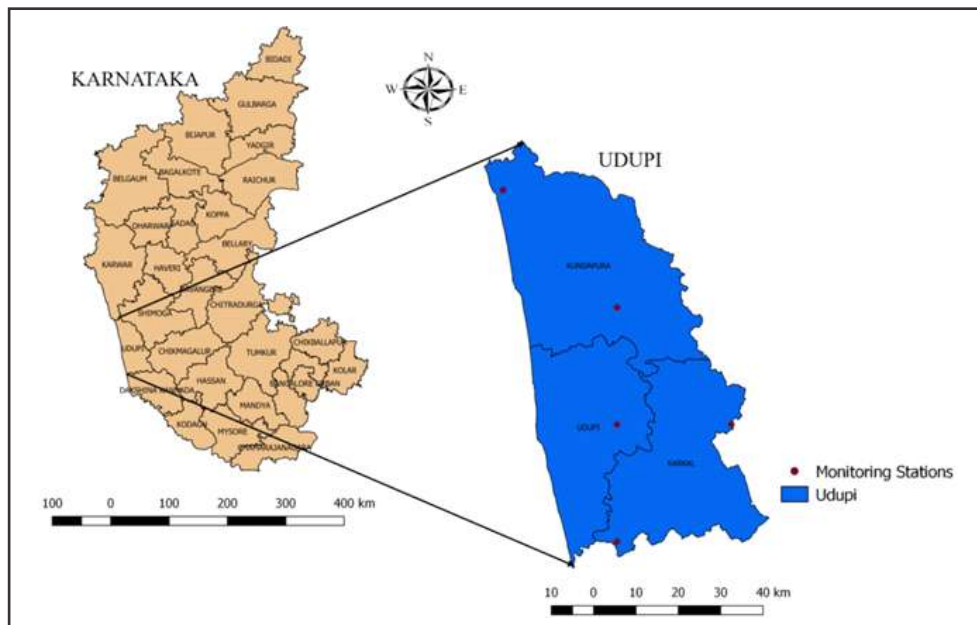
**Fig. 1:** Geographic location-Udupi District

### Data

Spatiotemporal cloud-free remote sensing data of Landsat sensors (1990-2020) has been downloaded from the USGS-Earth explorer data portal. The Landsat data (all bands including the thermal band) were geo-registered to a common Universal Transverse Mercator coordinate system and resampled to 30 m using the nearest neighbour algorithm. Field data for LU classification and validation was collected using a pre-calibrated Global Positioning System (GPS). The data from Google Earth for various classes like forest, plantation, agriculture, urban, water and open spaces were also collected and used during analysis and validation. The temperature data of 2018 was taken from KSNDMC (Karnataka State Natural Disaster Monitoring Centre), used for LST validation. Global air temperature data (at 2 m from ground-based on climate modeling grid of 0.25) was used to validate LST maps for 1990. A 10 km daily meteorological dataset of 0.25 deg grid was used to validate LST of 1990. The dataset is based on the NCEP-NCAR reanalysis (https://psl.noaa.gov/data/gridded/data.ncep.reanalysis.pressure.html#) merged with the University of East Anglia Climate Research Unit (CRU) monthly gridded temperature product and the NASA Langley Surface Radiation Budget (SRB-https://asdc.larc.nasa.gov/project/SRB) product and the data are available in 'NetCDF' format with one file per variable per year. Population data of 1901, 2001, and 2011 were collected from the Census of India (https://censusindia.gov.in/). Geological data such as soil, lithology, and agro-ecological zones were obtained from ICAR- NBSS & LUP (National Bureau of Soil Survey and Land Use Planning). Elevation data was obtained from USGS EROS Archive - Shuttle Radar Topography Mission (SRTM) of 30-meter resolution. Terrain analysis was carried out for obtaining slope. Rainfall data was obtained from World Clim- Global Climate Data version-2 (gridded climate data) with a spatial resolution of about 1 km$^2$.

### Method

The present study has been carried out in three phases (i) using remote sensing data to analyse forest ecosystem extent and conditions (fragmentation), (ii) identify and prioritize conservation importance regions or ecologically sensitive regions based on ecology, geo-climatic, land, and social attributes, (iii) quantifying LST and evaluating the relationship between CIR and LST.

LU analysis involved,

i.   Quality parameters: The remote sensing data were chosen to be devoid of or minimal cloud cover (less than 10 per cent) and pixel quality.

ii.  Image pre-processing and geo-referencing: The data was rectified radiometric errors and geometric errors. Geometric rectification is done using ground control points with the nearest neighborhood technique. The geo-rectified image is then projected to WGS/UTM 43N (EPSG: 32643).

iii. LU Classification: Remote sensing data is classified using a supervised classifier based on the Gaussian Maximum Likelihood algorithm. In the supervised technique, training data of representative LU describing the spectral attributes

(Lillesand *et al.*, 2014) is considered. The technique essentially considers variance and covariance of unknown pixels - (Reddy, 2009; Ganasri and Dwarakish, 2015; Ramachandra and Bharath, 2019b).

iv. Validation of LU information: Classified LU information is validated by accuracy assessment through computation of error matrix and Kappa statistics. Error matrix compares, on a category-by-category basis, the relationship between ground truth data (reference data) and the corresponding results of the classified data. Kappa coefficient measures the difference between the actual agreement between the reference data and classified data and is estimated through equation 1.

$$K = \frac{\text{Observed Accuracy-Chance Aggrement}}{\text{1-Chance Aggrement}} \quad \text{.......1}$$

**Evaluating ecosystem condition**

The condition of the forest ecosystem is assessed through fragmentation analyses involving both the extent of the forest and its spatial pattern. Fragmentation of forests measures the degree to which forested areas are broken into smaller patches and pierced with non-forest cover. It is estimated through the computation of $P_f$ and $P_{ff}$. $P_f$ is the ratio of the number of pixels that are forested to the total number of non-forested non-water

pixels in the kernel (3 × 3) and $P_{ff}$ is the proportion of all adjacent (in all cardinal directions) pixel pairs that include at least one forest pixel, for which both pixels are forested. Various levels of fragmentation consist of five components: (i) Interior forest: It is essentially consisting of thick forest cover, (ii) Patch forest: Forest area comprising small forested areas surrounded by non-forested land cover, (iii) Perforated forest: Forest pixels forming the boundary between an interior forest and relatively small clearings (perforations) within forest landscape, (iv) Edge forest: Forest pixels that define the boundary between interior forest and large non-forested land cover features and (v) Transitional forest: Areas between edge type and non-forest types. If higher pixels are non-forest, they will be tending to non-forest cover with a higher degree of edge.

**Land Surface Temperature [LST] estimation**

LST is estimated using time series data from top-of-atmosphere brightness temperatures from the infrared spectral channels of a constellation of geostationary satellites. Its estimation depends on the albedo, vegetation cover, and soil moisture (Bharath *et al.*, 2013; Ibrahim *et al.*, 2016; Sahana *et al.*, 2016). LST influences the partition of energy between ground and vegetation and determines the surface air temperature. Retrieval of LST from Lands at 8 thermal data involves computation of radiance correction, reflectance
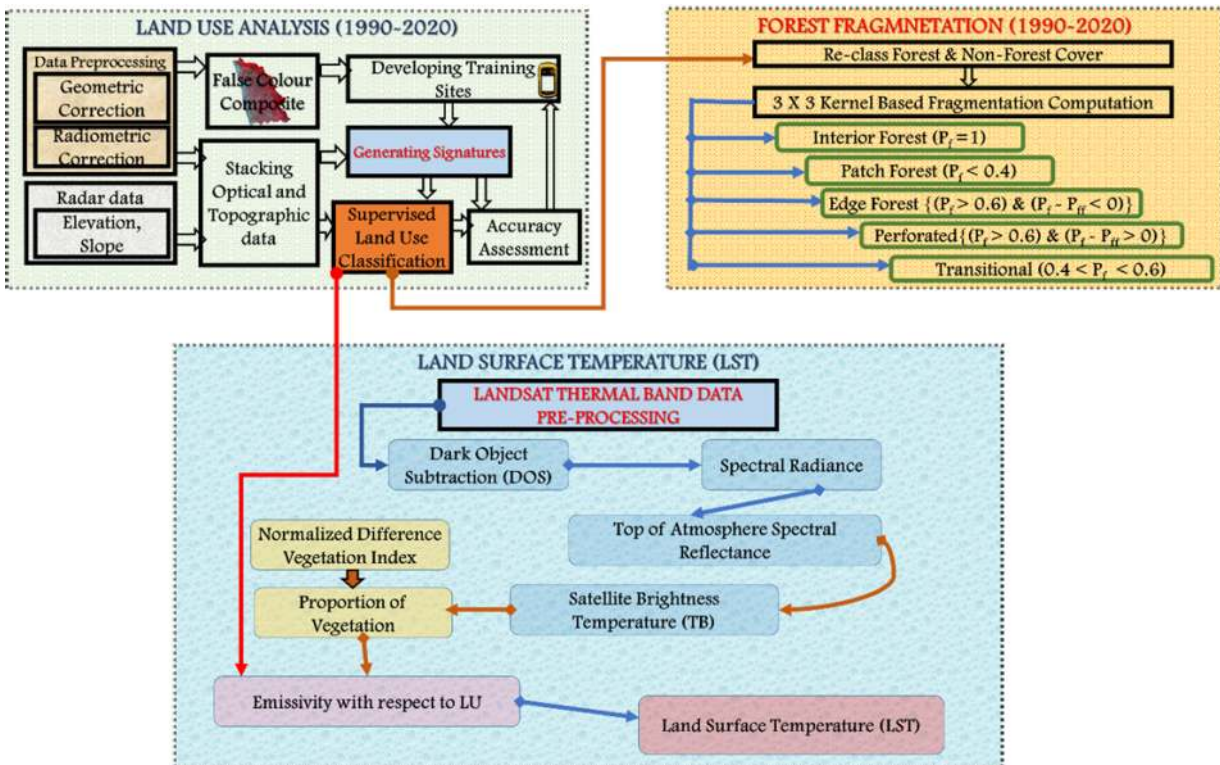


**Fig. 2:** Method adopted for LU, fragmentation, and LST analysis

**INDIAN FORESTER**

correction, converting DN value to brightness temperature, computation of NDVI, the proportion of vegetation. Emissivity-corrected LST as follows:

$$\text{Radiance correctness } L_\lambda = M_L Q_{cal} + A_L \quad .....2$$

$L_\lambda$ is TOA (temperature of atmosphere) spectral radiance (Watts/ (m$^2$ * srad * μm), $M_L$ is Band specific multiplicative rescaling factor from the metadata, $A_L$ is Band specific additive rescaling factor from the metadata, $Q_{cal}$ is Quantized and calibrated standard product pixel values (DN).

$$\text{Reflectance correctness } P\lambda' = M\rho Q_{cal} + A\rho \quad ......3$$

$P\lambda'$ is TOA (temperature of the atmosphere) planetary reflectance, $M\rho$ is Band-specific multiplicative rescaling factor from the metadata, $A\rho$ is Band-specific additive rescaling factor from the metadata.

$$\text{DN value converted to brightness temperature} \quad T_b = \frac{K_2}{\ln\left[\frac{K_1}{L_{10}} + 1\right]} \quad ......4$$

L10 is the spectral radiance of thermal band 10 [Wm−2sr−1μm−1], $T_b$ is the brightness temperature [Kelvin] and K 1 and K 2 are constants [Wm−2ster−1μm−1], K 1 = 666.09, K2 = 1282.71. Calculation of NDVI and Proportion of vegetation ($P_v$) using equations 5 and 6, respectively.

$$\text{NDVI} = \frac{\text{Band5 - Band4}}{\text{Band5 + Band4}} \quad ......5$$

Where Band5 is the near-infrared band and band4 is the red band.

$$P_v = \left(\frac{\text{NDVI-NDVI}_{min}}{\text{NDVI}_{max}\text{-NDVI}_{min}}\right)^2 \quad ......6$$

Land surface emissivity is very important for calculating LST as it is the proportionality factor that scales blackbody radiance (Planck's law) to predict emitted radiance, and it is the efficiency of transmitting thermal energy across the surface into the atmosphere (Kumari *et al.*, 2018). Emissivity is very close to 1 for all objects, but to get a precise temperature, emissivity values for each LC class is separately considered (Table 1). The land surface emissivity LSE (ε) is calculated as proposed by Sobrino *et al.*, (2004).

$$\varepsilon = 0.004P_v + 0.986 \quad ......7$$

**Table 1:** Table showing LU categories and emissivity values

| Land use types | Emissivity values |
|---|---|
| Densely urban | 0.946 |
| Forest cover | 0.985 |
| Non-forest cover | 0.950 |
| Water | 0.990 |

where ε is the emissivity.

$$\text{Emissivity-corrected LST in degrees Celsius} \quad T_b = \frac{T_b}{\{1+\left[\left(\frac{\lambda T_b}{\rho}\right)\ln\varepsilon\lambda\right]\}} \quad ......8$$

$\rho = h\frac{c}{\sigma}$ = 1.438*10$^{-2}$mK Where $\sigma$ is the Stefan-Boltzmann constant (1.38*10−23*J/K*), h is the Planck's constant (6.626*10−32*Js*), and c is the velocity of light (2.998*108*m/s*). Retrieval of LST from Lands at TM is as follows,

$$\text{Radiance correctness } L\lambda = \left(\frac{\text{Lmax - Lmin}}{\text{Qcal}_{max} - \text{Qcal}_{min}}\right) * (\text{Qcal - Qcal}_{min}) + \text{L}_{min} \quad ......9$$

$L_\lambda$ is temperature of atmosphere spectral radiance

Qcal is the quantized and calibrated standard product pixel value (DN)

$$\text{DN value converted to brightness temperature} \quad T_b = \frac{K_2}{\ln\left[\frac{K_1}{L_\lambda} + 1\right]} \quad ......10$$

$L_\lambda$ is the spectral radiance of thermal band 6 [Wm−2sr−1μm−1], is the brightness temperature [Kelvin] and K 1 ad K 2 are constants [mW*cm-2* sr-1], K 1 = 1260.56, K2 = 607.76.Emissivity corrected final LST will be computed using equation 7.

**Prioritization of Conservation Importance Regions (CIR)**

CIR refers to the areas of high ecological significance value. These are the regions where anthropogenic activities can cause alterations in the natural structure of the biological communities and natural habitats. The steps followed during identification and prioritization of CIR are detailed in Fig. 2 and listed below:

i. Creation of grids: The study area is divided into grids of 5' X 5' covering approximately 9 X 9 km$^2$ (comparable to grids of the Survey of India topographic maps of scale 1:50000) for prioritizing CIR at decentralized levels (panchayat level).

ii. Integration of data with grid: In this study, four different attributes namely ecology, geo-climatic, land, and social were selected for the prioritization of CIR. Ecology consists of flora and fauna present in the region. Geo-climatic parameters refer to the various geological and climatic parameters such as rainfall, elevation, slope, LST, soil, agro-ecological zones, and lithology. Finally, land essentially consists of forest cover and interior forest extent and social, composed of tribal and social population density.

iii. Weightage metric score: Weightages were assigned to attributes based on their significance value. The weightage metric score is estimated using equation 11.

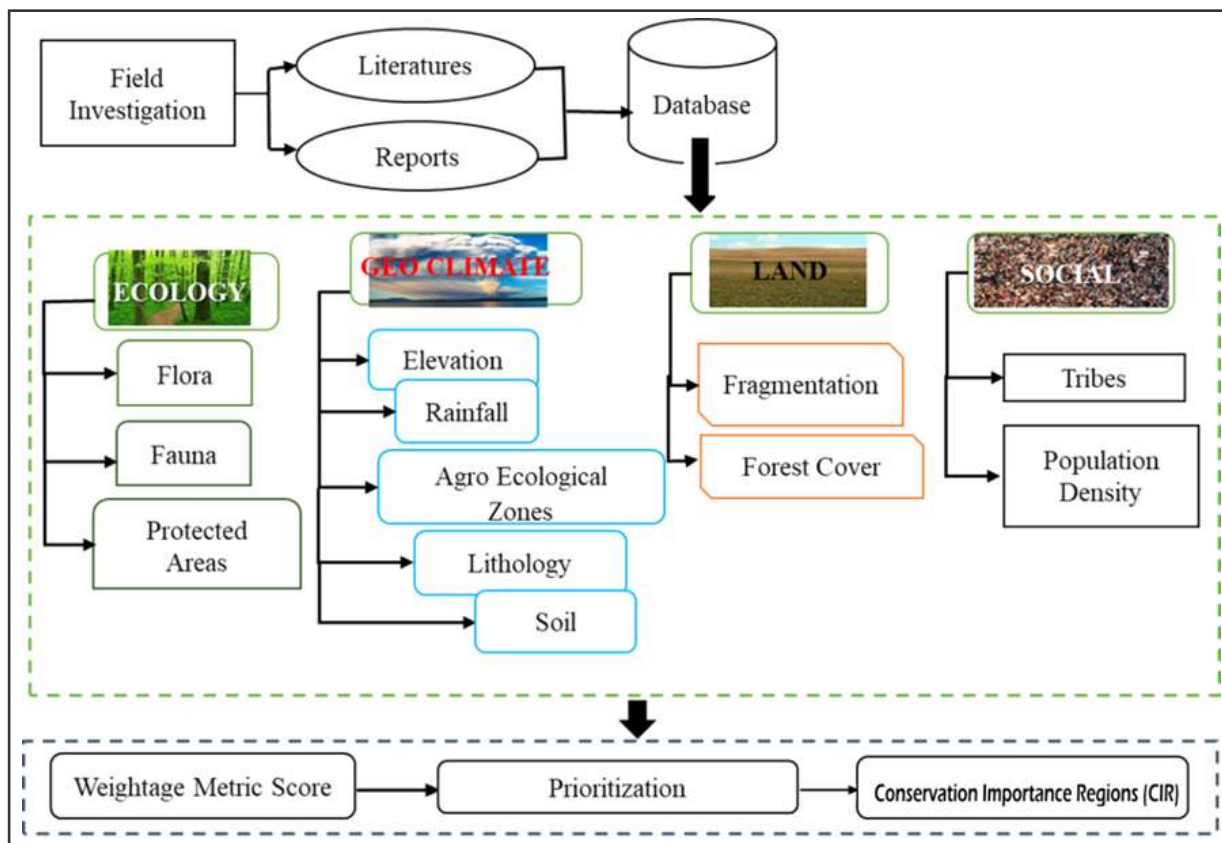$$\text{Weightage} = \sum_{i=1}^{n} W_i V_i \quad ......11$$

**Fig. 3:** Method adopted for prioritizing CIR

Where n is the number of data sets (variables), $V_i$ is the value associated with criterion i, and $W_i$ is the weight associated with that criterion. Based on the weightage, rank is given between 1 to 10 wherein value 10 corresponds to the highest priority for conservation, 7, 5, and 3 corresponds to high, moderate, and low level of prioritization, whereas 1 corresponds to least priority for conservation.

i.    Prioritization of CIR: Weights are aggregated for each grid and grouped into four groups as CIR 1, CIR 2, CIR 3 and CIR 4 based on the aggregated scores (CIR 1: aggregated scores > $\mu+2\sigma$, CIR 2 (for grids within $\mu+2\sigma$ and $\mu+\sigma$), CIR 3 (for grids with $\mu+\sigma$ and $\mu$) and CIR 4 (grids with values < $\mu$). In

particular, the weightages are based on an individual proxy and depends extensively on GIS techniques, which is the most effective method.

**Results**

*Landscape condition analysis*

Spatiotemporal quantification of LU transitions in Udupi for 1990-2020 was performed using the Maximum Likelihood Classification algorithm and accuracy of the classified map was analyzed by estimating kappa value and overall accuracy. LU map of Udupi has been shown in Fig. 3. The built-up area in the coastal region increased from 1485 hectares to 33,052.53 hectares, of 8.81% during the three decades. Area under forest cover

**Table 2:** Land uses in Udupi District (1990-2020)

| S.No. | Land Use Categories | 1990 | | 2018 | | 2020 | |
|---|---|---|---|---|---|---|---|
| | | (Ha) | (%) | (Ha) | (%) | (Ha) | (%) |
| 1 | Evergreen forest | 42,068.79 | 11.74 | 40,798.62 | 11.38 | 40,178.33 | 11.21 |
| 2 | Deciduous forest | 37,466.19 | 10.46 | 29,999.97 | 8.37 | 32,835.18 | 9.16 |
| 3 | Horticulture | 1,31,933.07 | 36.82 | 1,56,911.94 | 43.77 | 1,51,911.94 | 42.39 |
| 4 | Forest Plantations | 5,090.76 | 1.42 | 7,265.25 | 2.03 | 7,265.25 | 2.03 |
| 5 | Croplands | 1,20,544.83 | 33.64 | 90,132.75 | 25.14 | 1,04,305.67 | 29.11 |
| 6 | Built up | 1,485.72 | 0.41 | 11,069.64 | 3.09 | 33,052.53 | 9.22 |
| 7 | Water | 6,511.77 | 1.82 | 6,309.27 | 1.76 | 8,966.06 | 2.50 |
| 8 | Open lands | 6,635.25 | 1.85 | 6,162.57 | 1.73 | 10,136.03 | 2.83 |
| 9 | Scrub forest | 6,612.30 | 1.85 | 9,698.67 | 2.73 | 9,876.02 | 2.76 |
| | **Total** | | | | | **3,58,348.68** | |
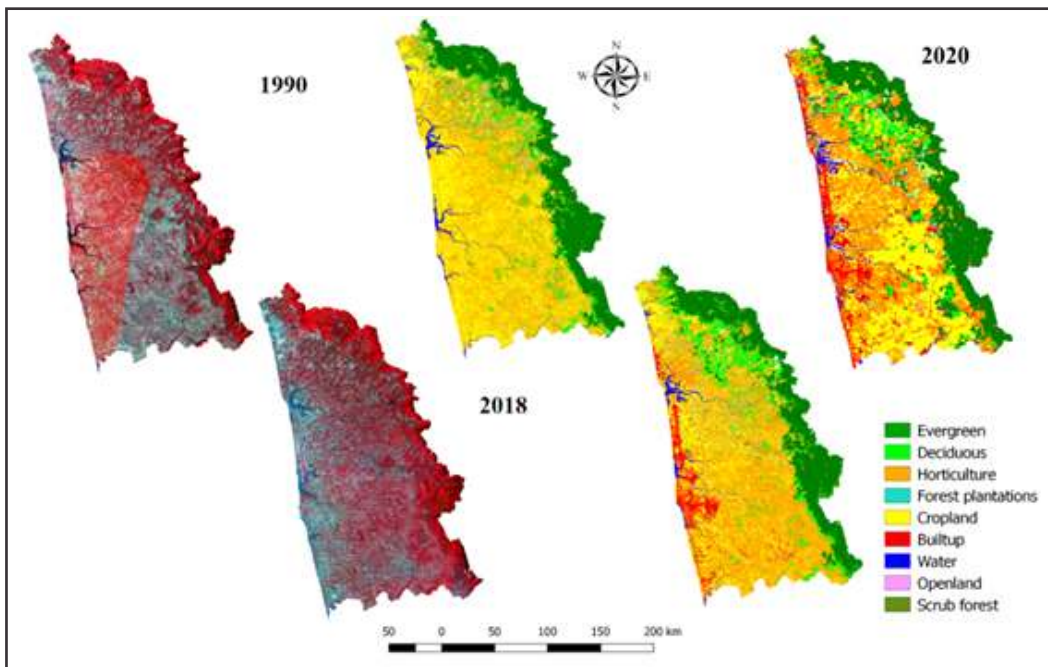
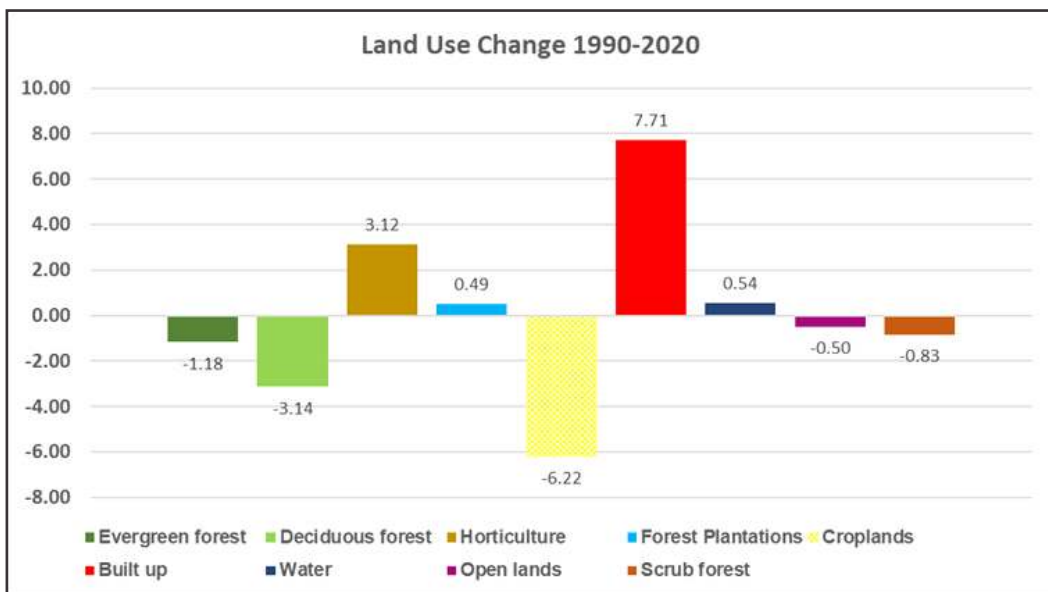**Fig. 4:** LU analysis of Udupi from 1990 to 2020



**Fig. 5:** Percentage change in LU analysis of Udupi during (1990-2020)

**Table 3:** Fragmentation Analysis of Udupi District (1990-2020)

| S.No. | Components | 1990 | | 2018 | | 2020 | |
|---|---|---|---|---|---|---|---|
| | | (Ha) | (%) | (Ha) | (%) | (Ha) | (%) |
| 1 | Non-forest | 2,66,144.67 | 74.27 | 2,71,530.63 | 75.77 | 2,80,373.84 | 78.24 |
| 2 | Patch | 3573.9 | 1.00 | 2124.18 | 0.59 | 1524.18 | 0.43 |
| 3 | Transitional | 6339.15 | 1.77 | 6738.39 | 1.88 | 3738.39 | 1.04 |
| 4 | Edge | 2713.59 | 0.76 | 3174.84 | 0.89 | 3174.84 | 0.89 |
| 5 | Perforated | 12,963.24 | 3.62 | 12,492.45 | 3.49 | 10,492.45 | 2.93 |
| 6 | Interior | 60,102.36 | 16.77 | 55,978.92 | 15.62 | 50,078.92 | 13.97 |
| 7 | Water | 6,511.77 | 1.82 | 6,309.27 | 1.76 | 8966.05 | 2.50 |
| | **Total Area** | | | | | **3,58,348.68** | |
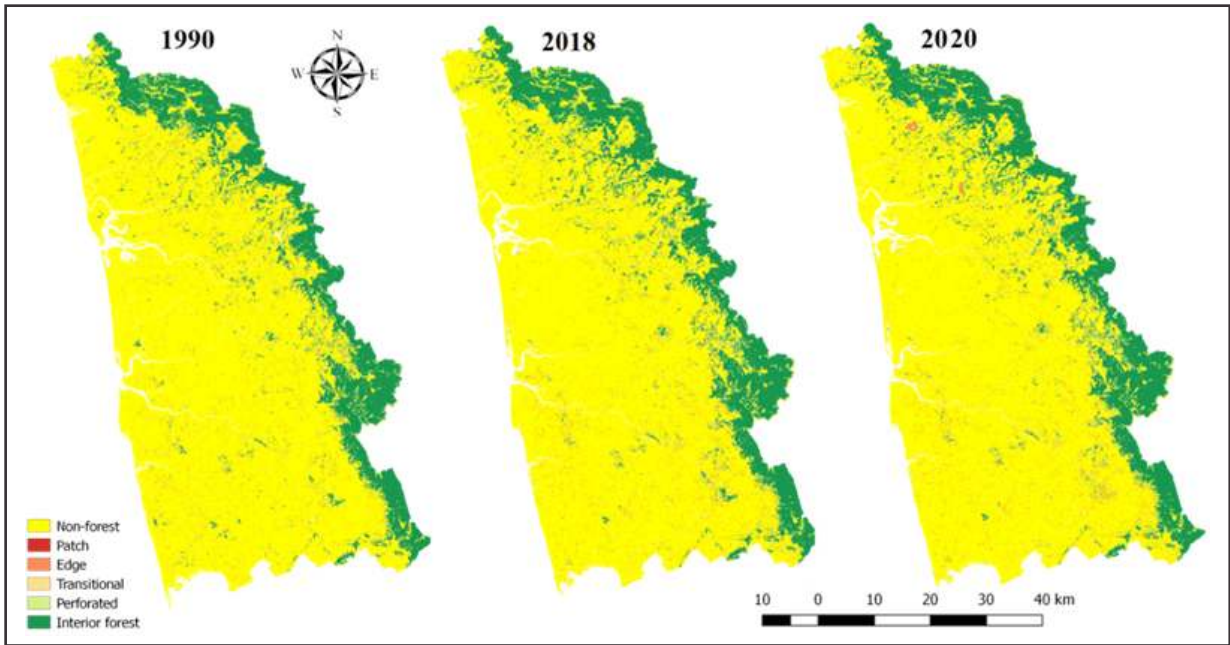
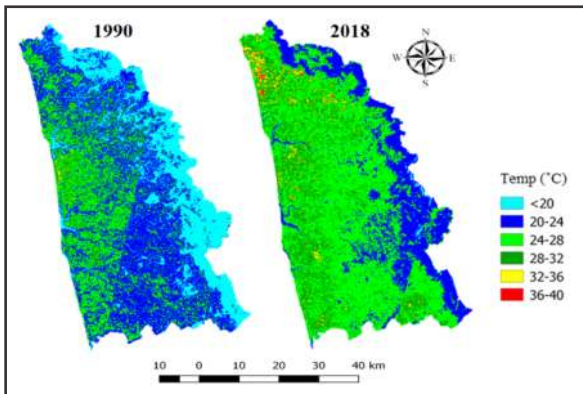**Fig. 6:** Fragmentation analysis of Udupi from 1990 to 2020



**Fig. 7:** Temporal dynamics of LST of Udupi from 1990-2018

*i.e.*, evergreen and deciduous has decreased from 11.74%, 10.47% (1990) to 11.21%, 9.16% (2020) respectively. Scrub forest increased from 1.85% (1990) to 2.76% (2020).The conversion of agricultural land to commercial use along the major highways has increased the built-up area. Horticulture plantations increased from 36.86% to 43.77% with rubber plantations during three decades (Table 2).

Fig. 4 illustrates that scrub forest increase by 1.37%, and built-up areas increased by 7.17%. Horticulture plantations replaced agricultural activities during three decades.

Fragmentation analyses show loss of intact forest (core) and Fig. 5 depicts fragmentation from 1990 to 2020. Table 3 gives the spatial extent of various types of fragments (interior non-forest, patch forest, transitional forest, edge forest, perforated forest, and interior forest). Area under interior forest has decreased from 16.77% (1990) to 13.97% (2020) while non-forest areas has increased from 74.27% (1990) to 78.24% (2020). The transitional forest has decreased from 1.8% (1990) to 1.04% (2020), with increased edge forests indicating the boundary between interior forest and non-forest has increased. The increase in non-forest areas signifies a major portion of the forest area has been converted into built-up areas, croplands, roads, etc. The core forest exists only as protected areas, sanctuaries, national parks, and sacred groves.

**Land Surface Temperature [LST]**

The higher temperature can be seen especially in non-forest areas due to an increase in built-up areas.

**Table 4:** Temperature Analysis of Udupi District (1990-2018)

| S. No. | Land use categories | 1990 | | | | 2018 | | | | Change (˚C) |
|---|---|---|---|---|---|---|---|---|---|---|
| | | Area (%) | Temp (˚C) | | | Area (%) | Temp (˚C) | | | |
| | | | Min | Max | Mean | | Min | Max | Mean | |
| 1 | Forest | 23.95 | 19.38 | 29.47 | 24.43 | 20.31 | 22.68 | 38.94 | 30.81 | 6.39 |
| 2 | Non-forest | 73.82 | 19.39 | 31.9 | 25.65 | 74.70 | 23.69 | 38.99 | 31.34 | 5.70 |
| 3 | Urban | 0.42 | 22 | 30.71 | 26.36 | 3.18 | 24.38 | 37.51 | 30.95 | 4.59 |
| 4 | Water | 1.82 | 20.68 | 28.65 | 24.67 | 1.81 | 23.27 | 37.17 | 30.22 | 5.56 |

The temporal LST analysis shows hilly regions are with moderate surface temperatures, evident from Table 4. Urban areas show an increase in temperature (maximum) from 30.71$^0$C (in 1990) to 37.51$^0$C (in 2018). Due to a reduction in the interior or intact forest cover, there is an increase in temperature from 29.47$^0$C (in 1990) to 38.94$^0$C (in 2018). Table 4 also illustrates the change in temperature across land-use categories over the period. The maximum change in temperature was observed over forest cover (with the fragmentation of forests) by 6.39$^0$C followed by non-forest cover by 5.70$^\circ$C during the past 28 years, comparable with ground data.

### Conservation Importance Regions (CIR)

Compilation of attribute data related to ecology, geo-climate, land, and social aspects has been collected, and aggregated weight has been computed.

### *Ecology*

The ecosystem's health is assessed based on key variables such as conservation status, diversity, etc. Data is compiled from the field, review of published literature, and virtual data portals (such as avibase, -found butterflies, etc.). Conservation Reserves (CR) have been established under Protected Areas under the Wildlife Amendment Act of 2002. Conservation Reserves are essentially the buffer zone between National Parks (NP), Wildlife Sanctuaries, and reserve forests. Higher weights were assigned to CR and NP,

and the grids with the critically endangered and endangered species were assigned a value of 10, vulnerable and near-threatened species are assigned a value of 7, threatened species is assigned 5, common, data deficient, rare and lower risk were assigned a value of 3 while not evaluated is assigned a value of 1. Fig. 6a-h depicts the distribution of flora and fauna with conservation status and weights, which shows most of the species are concentrated across wildlife sanctuaries in the district.

The flora of Udupi district has been compiled by reviewing published literature and data portals. The district is home to critically endangered species such as *Elaeocarpus gaussenii, Syzygium travancoricum, Utleria salicifolia, Vateria indica, Vatica chinensis* and vulnerable species such as *Chloroxylon swietenia, Cinnamomum sulphuratum, Dalbergia latifolia, Garcinia indica, Myristica malabarica, Ochreinauclea missionis, Paracautleya bhatii, Santalum album, Saraca asoca, Saraca indica.* The dominant families are Fabaceae, Lamiaceae, Dipterocarpaceae, Euphorbiaceae.

Udupi district has rich faunal diversity. The region has near-threatened amphibian species such as *Philautus beddomii, Ramanella montana, Rana curtipes, Tomoptema rufescens,* and vulnerable species such as *Ichthyophis beddomei, Micrixalus saxicola, Nyctibatrachus major, Philautus glandulosus, Rana aurantiaca, Rana leithi.* Mammals species such as *Bos*



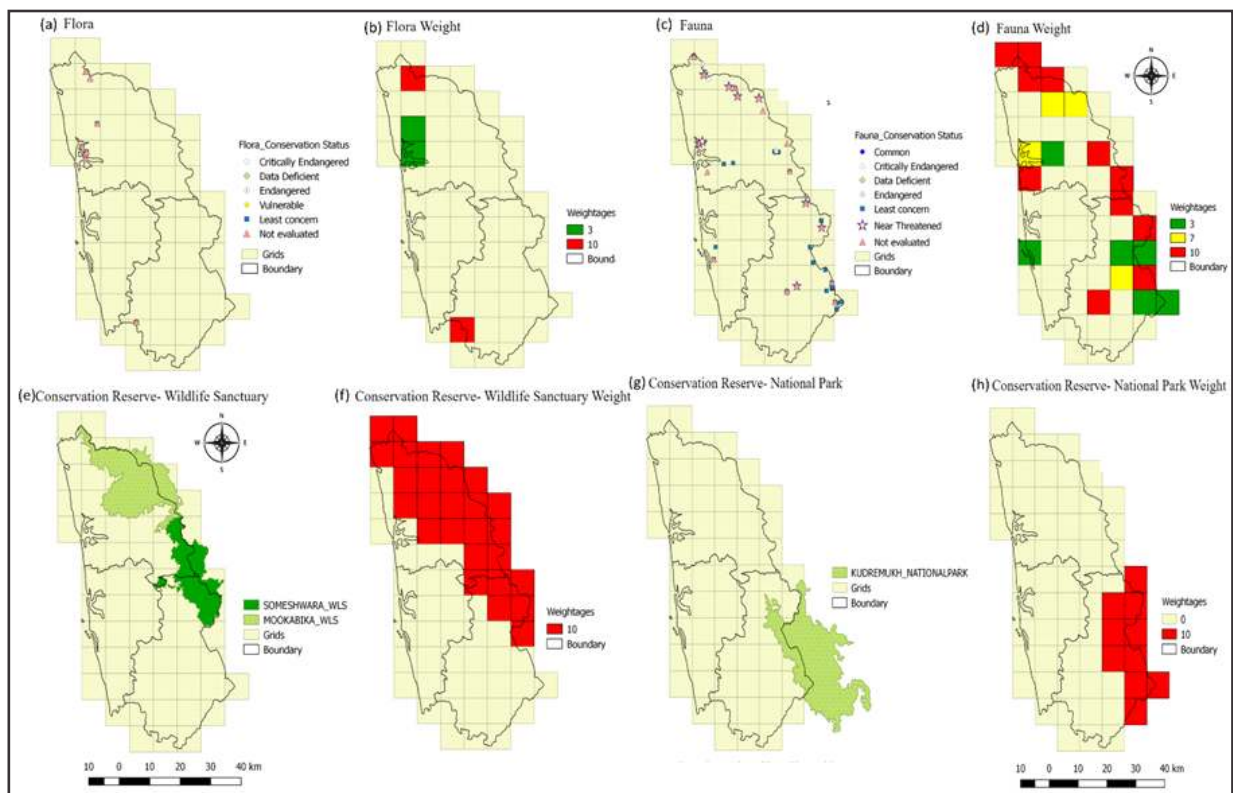**Fig. 8:** Ecological variables with their weights

gaurus, *Cervus unicolor, Funambulus subineatus, Melursus ursinus, Neophocaena phocaenoides, Physeter macrocephalus* are under near threatened and species *Hyaena hyaena, Lutralutra, Panthera pardus, Ratufa macroura, Sousa chinensis* are under vulnerable category of IUCN conservation status. The district has critically endangered birds such as *Fregata andrewsi, Gyps bengalensis, Gyps indicus, Sarcogyps calvus* and vulnerable category birds such as *Chaetornis striata, Ciconia episcopus, Clanga clanga, Clanga hastata, Columba elphinstonii, Gallinago nemoricola, Leptoptilos javanicus, Schoenicola platyurus.* The district has vulnerable category reptiles such as *Cnemaspis indica, Cnemaspis indraneildasi, Cnemaspis jerdonii, Hemidactylus albofasciatus, Hemidactylus sataraensis, Kaestlea laterimaculata, Melanophidium bilineatum, Oligodon brevicauda, Uropeltis phipsonii.*

Kudermukh National Park covers a minor portion of the study region and shares its boundary with Dakshina Kannada. The study region has diverse flora and fauna: 162 species of flowering plants representing 50 families. Fabaceae had maximum tree species (23), followed by Rhizophoraceae (17 species), Moraceae (7 species) – known as the family of figs and keystone species for plants, etc. *Vateria indica* is one of the critically endangered species present in the district while *Hopea ponga,* and *Syzygium caryophyllatum* are the two endangered species, and *Garcinia indica,* and *Ochreinauclea missionis* are the two vulnerable species that are well distributed in the district. Someshwara and Mookambika wildlife sanctuary are known for the variety of birds and wild flowering species endemic to the region. 816 species of fauna representing 123 families were documented. Malabar Grey Hornbill, Small Green
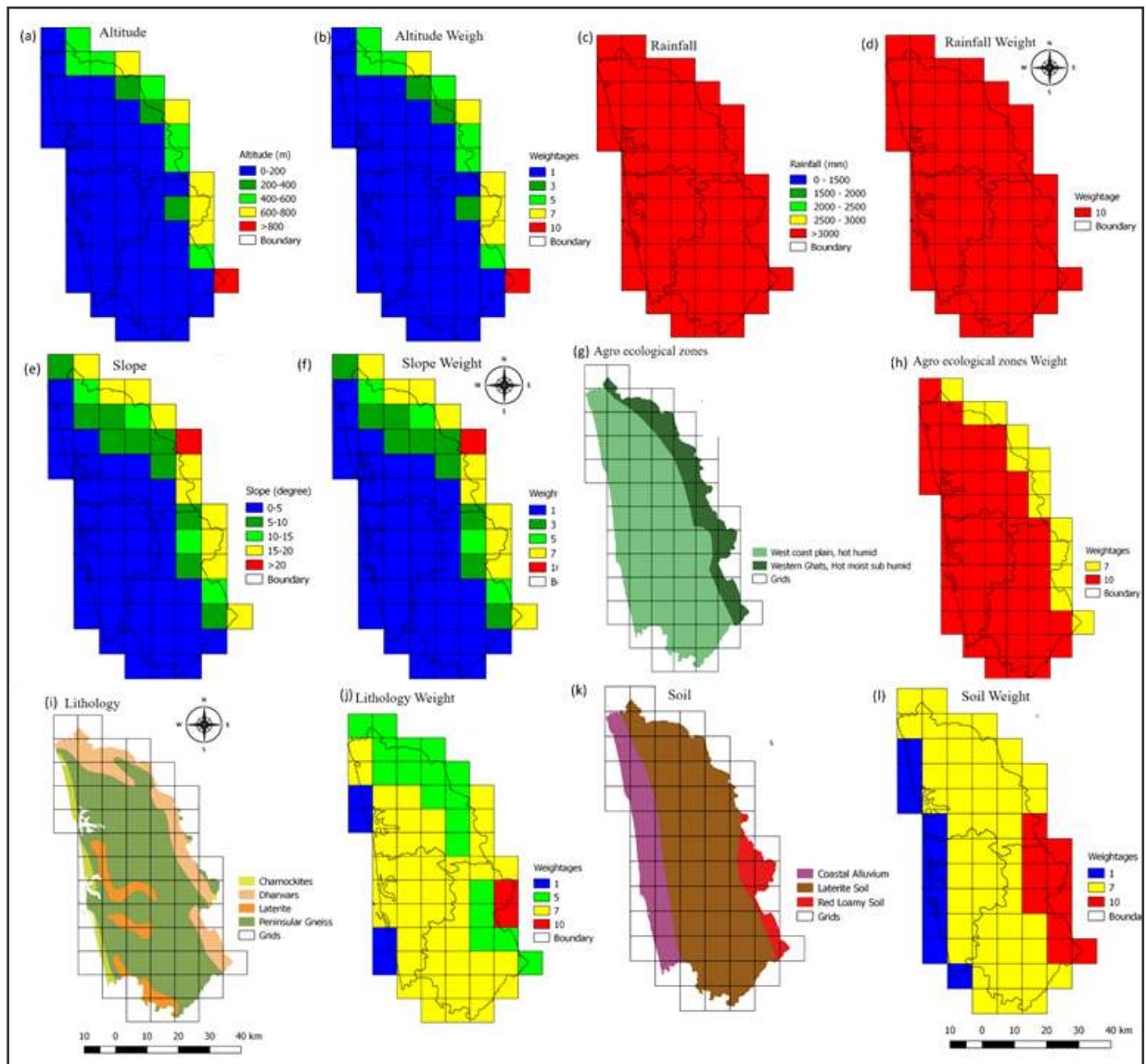


**Fig. 9:** Geo-climatic factors and their weight

Barbet, Gotyla, Rock Bush Quail, Grey Jungle fowl, Malabar Wood shrike, Indian Rufous Babbler, Nilgiri Thrush, Nilgiri Blue Robin, Day's Glass Fish, Gunther's catfish, Tyler's Leaf Warbler, etc., are found in the district.

### Geo-climate

The geo-climatic parameter plays a crucial role in determining the landscape dynamics of any region. Fig. 7a-l depicts the different geo-climatic parameters in the region and their weights assigned to the grids. The patterns of altitude, slope, rainfall helps in determining the forest cover, biodiversity, etc., of a region. The rainfall pattern shows entire district receives high rainfall during all seasons. The coastal part falling under a hot moist sub-humid region can be attributed to a favorable climatic pattern for healthy vegetation. Grids with high rainfall and soil types have rich forest cover with high biodiversity and conservation values. Regions with high rainfall, elevation, and slope were assigned a value of 10, and the lowest is given a value of 1. Loamy soil is considered best for agricultural purposes with rich porosity and humus content, which is assigned a value of 10, while laterite and mixed red and black soil are assigned a value of 7, red sandy and medium black were given 5 and coastal alluvium as 1. Lithology is an important factor considering landscape structure and patterns. Charnockites was given the highest value of 10 followed by peninsular gneiss of 7, closepet granite, and Dharwars were assigned 5 while alluvium was assigned 1. Agro-ecological zones play a significant role in determining the climate of a region. Therefore, hot humid is assigned the highest value of 10 as the region receives high rainfall around 1500 mm or more. Hot moist sub-humid is assigned 7, hot dry sub-humid is given 5, and hot moist semi-arid is assigned the lowest value of 3.

### Land

Grids are prioritized based on the proportion of forest cover. Forest fragments were computed using standard protocol wherein interior core forest patches were considered devoid of any edge effects. Grids having more than 60% forest cover were assigned a value of 10, and accordingly, values were assigned. Land use analysis revealed that the region has about 2.98% under evergreen forest. Most parts are with less than 15% forest cover. Expansion of agricultural activities and the introduction of exotic species has led to the destruction of large forest patches at a temporal scale. The coastal taluks have a forest cover of less than 15%. Fig. 8 depicts the weights assigned to the grids based on the extent of forest cover. Fragmentation analysis revealed that 3.39% of the area is under core interior forest while 94.25% area is under non-forest cover.

### Social

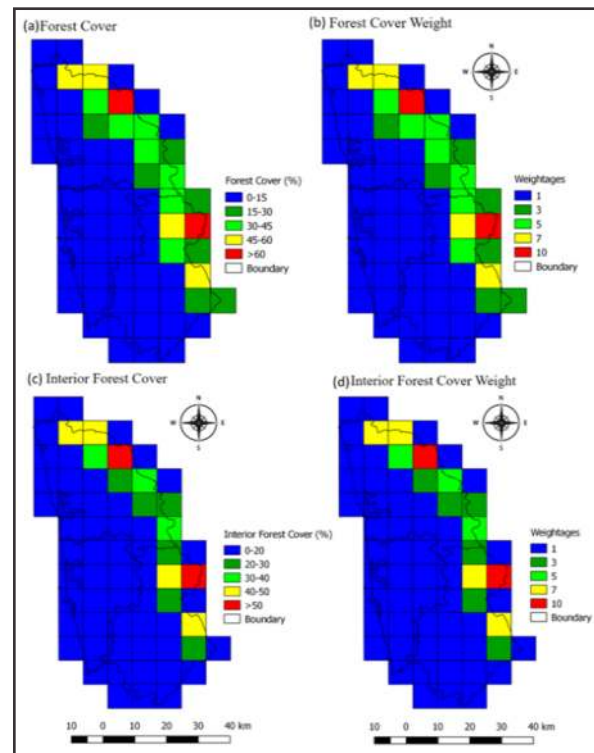Population increase often leads to degradation of natural resources. An increase in population density will
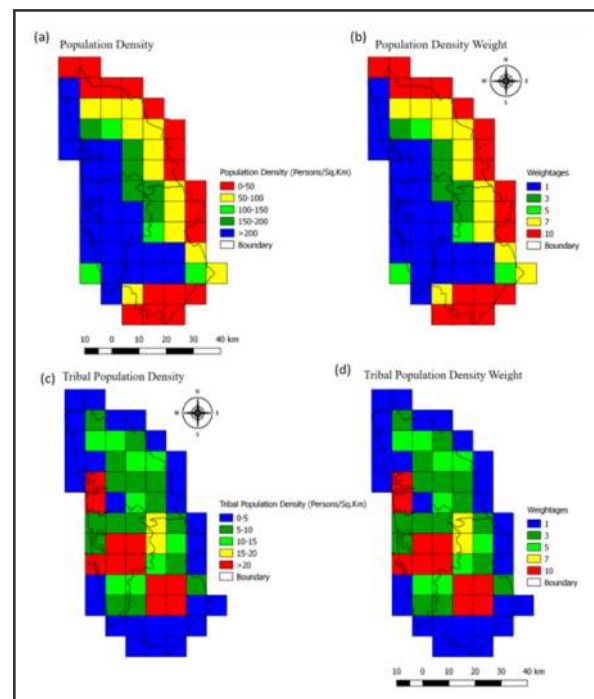


**Fig. 10:** Land condition factors and weight



**Fig. 11:** Social factors considered and weight

lead to loss of natural resources, species extinction, etc. In this study, population density per km$^2$ has been considered as one of the influencing factors in resource use. Therefore, grids with less population density were

given higher weights. Grid-wise, village population was computed for 2011. The grids with a population density of less than 50 persons were assigned high weights and vice-versa. Fig. 9 depicts the population density assigned to the grids with corresponding weights. The hilly regions have high forest cover with less population density. Forest dwellers (tribes) of the study regions were mapped, and the grids with a high tribal population were given higher weight. Forest dwellers were spatially mapped and were given higher weights as they are directly or indirectly dependent on forest resources and also protect the forest.

Based on the relative significance of themes, regions were prioritized using weightage metric score as CIR 1 (Regions of highest sensitivity), CIR 2 (Regions of higher sensitivity), CIR 3 (Regions of high sensitivity), and CIR 4 (Regions of moderate sensitivity). Spatially 15% of the district represents CIR1, while 31% of the area represents CIR2. 42% of the district represents CIR 3, and about 12% of the district is in CIR 4. Fig. 10 depicts with taluk and village boundaries. CIR analysis at the village level shows only 14 villages in CIR 1, 52 villages in CIR 2, 178 villages in CIR 3, and 51 in CIR 4 (Fig. 10).
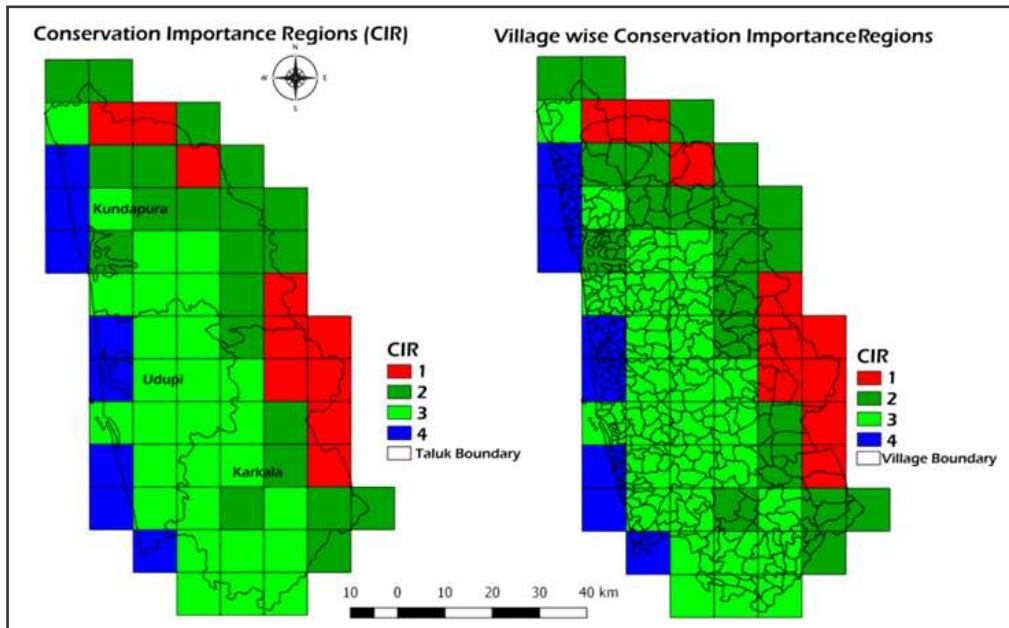


**Fig. 12:** CIR at taluk and village level- Udupi District
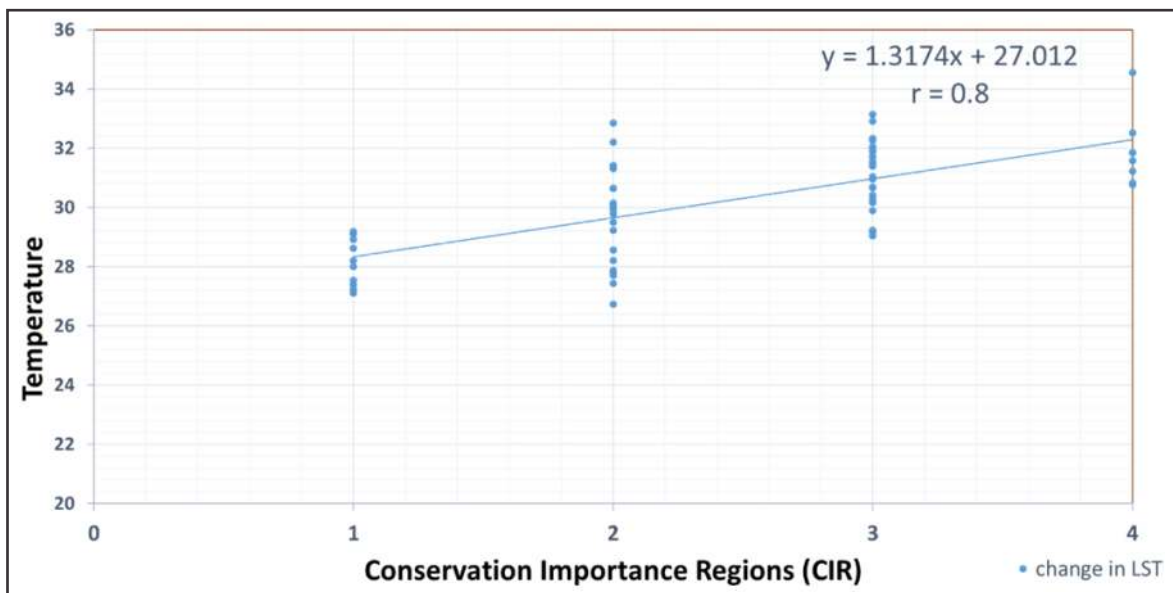


**Fig. 13:** LST across CIR- Udupi

CIR 1 has the maximum forest cover and rich biodiversity along with less population, which aided in the low LST. LST trend shows an increase in temperature (r = 0.8) across CIRs (Fig. 11).

## LST in conservation importance region (ecologically sensitive regions)

The ecological sensitiveness of a region has a direct impact on temperature. CIR 1 has a lower temperature compared to CIR 2 -4.

Multivariate analysis is carried out to determine the relationship between LST and various independent variables (rainfall, forest cover, interior forest cover, and population density). In the study, variables considered are rainfall weight $(x_1)$, forest cover $(x_2)$, interior forest cover $(x_3)$, and population density weight $(x_4)$ to understand the change of temperature across the CIR regions in the districts. The probable relationship is given by

$$LST = 0\,x_1 - 0.28x_2 + 0.16\,x_3 - 0.28\,x_4 + 31.94 \ (r: 0.851, p < 0.05)$$

## Conclusion

Either natural or induced by humans drive landscape dynamics with changes occurring in the physical space. LULC transitions leading to deforestation, which have altered the Western Ghats landscape structure. The anthropogenic activities have led to the loss of primeval forest cover due to monoculture plantations of exotic species. The comprehensive knowledge of CIR / ESR and prioritization is quintessential for evolving strategies of conservation. The study showed a loss in forest cover during 1990-2020, increasing urban and open surfaces. Horticulture plantations increased from 36.82% (1990) to 42.39% (2020). Conversion of agricultural land to commercial uses, all along the major highways, has increased the built-up area from 0.22% to 9.22%. Fragmentation analysis shows a decline in interior forests and an increase of non-forest areas. Temporal LST analysis across LU categories shows an increase in LST. It has been observed that urban areas show an increase in maximum temperature. Bio-Geo climatic, ecological, and social attributes were used for prioritizing and identification of CIR regions at disaggregated levels (grids). The study showed the variation in soil, lithology etc., across the districts and change in climate pattern with respect to chosen variables (Bio-geo climatic, ecological, hydrologic, and social). CIR analysis highlights that Udupi, a coastal districts shows, spatially 15% of the area represents CIR 1, while 31% of the area represents CIR 2. 42% of the area represents CIR 3 and about 12% of the area is in CIR 4. CIR 2 regions have sensitivity similar to CIR 1 and have the potential to become CIR 1 with appropriate eco-restoration strategies. CIR 1 and CIR 2 are the no-go area regarding developments, and CIR 4 is referred to as the least possible eco-sensitive region. The Community-based Conservation (CBC) of CIR 2 and 3 is proposed for the conservation of biological diversity (or wildlife) involving local communities in decision-making. The level of eco-sensitiveness directly impacts temperature with a correlation of 0.80 across eco-sensitive regions in Udupi.

## उड़ूपी जिला, कर्नाटक में संरक्षण महत्व के क्षेत्रों और वन परिवर्तनों का मूल्यांकन

टी.वी. रामचन्द्रा, भारथ सीत्तूरू और विनय एस.

### सरांश

वर्तमान अध्ययन में पारिस्थितिकीय, भू-जलवायवीय, भूमि और सामाजिक पहलुओं पर आधाारित उड़ूपी जिला, केन्द्रीय पश्चिमी घाटों में वियुक्त स्तर पर संरक्षण महत्व के क्षेत्रों को प्राथमिकीकृत किया गया है। संरक्षण महत्व क्षेत्र (सी आइ आर) अथवा पारिस्थितिकीय संवेदी क्षेत्र (ई एस आर) विशेष जैव और अजैव तत्वों के साथ विशिष्ट पारिस्थितिकीय इकाइयां हैं, जिन्हें सबसे अधिक देखभाल और पोषणीय विकास की जरूरत है। ग्रिड स्तरों (5' x 5' ग्रिड अथवा 9 x 9 कि.मी.) पर संरक्षण महत्व क्षेत्रों के प्राथमिकीकरण वन भूदृश्य गतिकी और योजना की बेहतर समझ के लिए स्थानिक निर्णय सहायता प्रणाली के तौर पर कार्य करते हैं। अल्पकालिक सूदूर संवेदी आँकड़ों का उपयोग करके वन भूदृश्य गतिकी के विश्लेषण मे वनावरण में कमी के साथ 8.8 प्रतिशत सब निर्मित इलाकों में वृद्धि को दर्शाया, जिसके फलस्वरूप 1990-2018 के दौरान उड़ूपी जिले में 4 डि.से. तक अधिकतय तापमान में वृद्धि हुई। भू सतह तापमान में भू दृश्य गति की भूमिका को समझने के लिए बहुविचार सांख्यिकीय विश्लेषण किया गया। सहसंबंध विश्लेषण r = 0-8 के साथ संरक्षण महत्व क्षेत्र में भू सतह तापमान के वर्तमान रुझान को दर्शाता है, जहाँ संरक्षण महत्व क्षेत्र 1 निम्नतम तापमान दर्शाता है और संरक्षण महत्व क्षेत्र 4 में अधिकतम तापमान था।

### References

Aronson J. and Alexander S. (2013). Ecosystem Restoration is Now a Global Priority: Time to Roll up our Sleeves. *Restor Ecol.*, **21**: 293–296. https://doi.org/10.1111/rec.12011.

Asgarian A., Amiri B.J. and Sakieh Y. (2015). Assessing the effect of green cover spatial patterns on urban land surface temperature using landscape metrics approach. *Urban Ecosyst.*, **18**: 209–222.

Bharath S., Rajan K.S. and Ramachandra T.V. (2013). Land Surface Temperature Responses to Land Use Land Cover Dynamics. *Geoinfor Geostat An Overv.*, **1**:. https://doi.org/10.4172/2327-4581.1000112.

Bonan G.B. (2008). Forests and Climate Change: Forcings, Feedbacks, and the Climate Benefits of Forests. *Science*, (80- ) **320**: 1444–1449. https://doi.org/10.1126/science.1155121.

Chakraborty S.D., Kant Y. and Mitra D. (2015). Assessment of land surface temperature and heat fluxes over Delhi using remote sensing data. *J. Environ Manage.*, **148**: 143–152.

Danodia A., Patel N.R. and Chol C.W. (2019). Application of S-SEBI model for crop evapotranspiration using Landsat-8 data over parts of North India. *Geocarto Int.*, **34**: 114–131.

Estoque R.C., Murayama Y. and Myint S.W. (2017). Effects of landscape composition and pattern on land surface temperature: An urban heat island study in the megacities of Southeast Asia. *Sci. Total Environ.*, **577**: 349–359.

Gadgil M., Daniels R.J.R. and Ganeshaiah K.N. (2011). Mapping ecologically sensitive, significant and salient areas of Western Ghats: proposed protocols and methodology. *Curr. Sci.*, 175–182.

Ganasri B.P. and Dwarakish G.S. (2015). Study of land use/land cover dynamics through classification algorithms for Harangi catchment area, Karnataka State, INDIA. *Aquat Procedia*, **4**: 1413–1420.

Hansen M.C., DeFries R.S., Townshend J.R.G. and Sohlberg R. (2000). Global land cover classification at 1 km spatial resolution using a classification tree approach. *Int. J. Remote Sens.*, **21**: 1331–1364.

Hansen M.C., Stehman S.V. and Potapov P.V. (2010). Quantification of global gross forest cover loss. *Proc. Natl. Acad. Sci.*, **107**: 8650–8655.

Huang C., Song K. and Kim S. (2008). Use of a dark object concept and support vector machines to automate forest cover change analysis. *Remote Sens. Environ.*, **112**: 970–985.

Ibrahim I., Samah A.A., Fauzi R. and Noor N.M. (2016). The land surface temperature impact to land cover types. *Int Arch Photogramm Remote Sens. Spat Inf. Sci.*, **41**: 871.

Jackson R.B. and Baker J.S. (2010). Opportunities and Constraints for Forest Climate Mitigation. *Bioscience*, **60**: 698–707. https://doi.org/10.1525/bio.2010.60.9.7.

Kayet N., Pathak K., Chakrabarty A. and Sahoo S. (2016). Spatial impact of land use/land cover change on surface temperature distribution in Saranda Forest, Jharkhand. *Model Earth Syst Environ.*, **2**: 1–10.

Kuemmerle T., Chaskovskyy O. and Knorn J. (2009). Forest cover change and illegal logging in the Ukrainian Carpathians in the transition period from 1988 to 2007. *Remote Sens Environ.*, **113**: 1194–1207.

Kumari B., Tayyab M. and Mallick J. (2018). Satellite-driven land surface temperature (LST) using Landsat 5, 7 (TM/ETM+ SLC) and Landsat 8 (OLI/TIRS) data and its association with built-up and green cover over urban Delhi, India. *Remote Sens Earth Syst Sci.*, **1**: 63–78.

Lawrence D. and Vandecar K. (2015). Effects of tropical deforestation on climate and agriculture. *Nat Clim Chang.*, **5**: 27–36. https://doi.org/10.1038/NCLIMATE2430

Le-Xiang Q., Hai-Shan C.U.I. and Chang J. (2006). Impacts of land use and cover change on land surface temperature in the Zhujiang Delta. *Pedosphere*, **16**: 681–689.

Leilei L., Jianrong F. and Yang C. (2014). The relationship analysis of vegetation cover, rainfall and land surface temperature based on remote sensing in Tibet, China. In: *IOP conference series: earth and environmental science*, p 12034.

Liang S., Wang D., He T. and Yu Y. (2019). Remote sensing of earth's energy budget: synthesis and review. *Int. J. Digit Earth*, **12**: 737–780.

Liu L., Jing X., Wang J. and Zhao C. (2009). Analysis of the changes of vegetation coverage of western Beijing mountainous areas using remote sensing and GIS. *Environ Monit Assess.*, **153**: 339–349.

Mohamed A.A., Odindi J. and Mutanga O. (2017). Land surface temperature and emissivity estimation for Urban Heat Island assessment using medium-and low-resolution space-borne sensors: A review. *Geocarto Int.*, **32**: 455–470.

Mujabar S. and Rao V. (2018). Estimation and analysis of land surface temperature of Jubail Industrial City, Saudi Arabia, by using remote sensing and GIS technologies. *Arab J., Geosci* **11**: 1–13.

Ramachandra T.V. and Aithal B.H. (2012). Land use dynamics at Padubidri, Udupi District with the implementation of large scale thermal power project. *Int J Earth Sci Eng.*, **5**: 409–417.

Ramachandra T.V. and Bharath S. (2019a). Global Warming Mitigation Through Carbon Sequestrations in the Central Western Ghats. *Remote Sens Earth Syst Sci.*, **2**: 39–63. https://doi.org/10.1007/s41976-019-0010-z.

Ramachandra T.V. and Bharath S. (2019b) Carbon Sequestration Potential of the Forest Ecosystems in the Western Ghats, a Global Biodiversity Hotspot. *Nat Resour Res.*, **29**: 2753–2771. https://doi.org/10.1007/ s11053-019-09588-0.

Ramachandra T.V., Bharath S. and Bharath A.H. (2020). Insights of Forest Dynamics for the Regional Ecological Fragility Assessment. *J Indian Soc Remote Sens.*, 48: 1169–1189. https://doi.org/10.1007/s12524-020-01146-z.

Ramachandra T.V., Bharath S. and Chandran M.D.S. (2016). Geospatial analysis of forest fragmentation in Uttara Kannada District, India. *For Ecosyst.*, **3**: 10. https://doi.org/10.1186/ s40663-016-00 69-4.

Ramachandra T.V., Bharath S., Chandran M.D.S. and Joshi N. V. (2018). Salient Ecological Sensitive Regions of Central Western Ghats, India. *Earth Syst Environ.*, **2**: 15–34.

Ramachandra T.V. and Bharath S. (2019c). Sustainable Management of Bannerghatta National Park, India, with the Insights in Land Cover Dynamics. *FIIB Bus Rev.*, **8**: 118–131. https://doi.org/10.1177/2319714519828462.

Ramachandra T. V. and Kumar U. (2010). Greater Bangalore: Emerging urban heat island. *GIS Dev*, **14**: 86–104.

Ramachandra T.V., Tara N.M. and Bharath S. (2017). Web based spatial decision support system for sustenance of western ghats biodiversity, ecology and hydrology. Creat Congition Art Des Ed by Aneesha Sharma Jamuna Rajeswaran, 58–70.

Ramachandra T.V., Vinay S. and Bharath S. (2021) Visualisation of landscape alterations with the proposed linear projects and their impacts on the ecology. *Model Earth Syst Environ.*, 1–13.

Reddy M.B. (2009). Land cover classification using IRS LISS III satellite image and Digital Elevation Model in hilly environment- a case study in Nongkhyllem Wildlife Sanctuary, Meghalaya. *Indian Forester.*, **135**: 487–499.

Sahana M., Ahmed R. and Sajjad H. (2016). Analyzing land surface temperature distribution in response to land use/land cover change using split window algorithm and spectral radiance model in Sundarban Biosphere Reserve, India. *Model Earth Syst Environ.*, **2**: 81.

Shwetha H.R. and Kumar D.N. (2016). Prediction of high spatio-temporal resolution land surface temperature under cloudy conditions using microwave vegetation index and ANN. *ISPRS J. Photogramm Remote Sens.*, **117**: 40–55.

Xianhong Q. (2015). Eco-Sensitivity assessment and protection policy in a complex geomorphic region in China. *J. Resour Ecol.*, **6**: 44–51.

Zhu W., Jia S., Lü A. and Yan T. (2012). Analyzing and modeling the coverage of vegetation in the Qaidam Basin of China: The role of spatial autocorrelation. *J. Geogr Sci.*, **22**: 346–358.